Double-Filtering Performance of Acousto-Optic Tunable Filter with Two Crystals

Huang Junfeng Wang Hao Zhang Chunguang Gao Qiang

Fujian Provincial Key Laboratory for Photonics Technology, Key Laboratory of Optoelectronic Science and Technology for Medicine of Ministry of Education, College of Photonics and Electronic Engineering, Fujian Normal University, Fuzhou, Fujian 350007, *China*

Abstract The noncollinear acousto-optic tunable filter (AOTF) is a new type of spectral component that is developed according to the abnormal acousto-optic interaction principle. The spectral resolution and sidelobe of diffraction signal are two important indices for evaluating the performance of AOTF. The basic principle of double-filtering using two AOTFs is described. The experimental results confirm that the double-filtering achieves a 40.4% to 83.2% improvement in the spectral resolution and from 9.5570 dB to 13.2407 dB suppression of the sidelobes. The results of this exploratory study demonstrate that double-filtering using two AOTFs has great potential for application in the field of the acousto-optic filtering.

Key words optical devices; acousto-optic tunable filter; spectral resolution; sidelobe; double filtering

OCIS codes 230.1040; 230.7408; 050.1940

声光可调滤波器双晶体二次滤波的性能分析

黄峻峰 王 号 张春光 高 强

福建师范大学光电与信息工程学院医学光电科学与技术教育部重点实验室, 福建省光子技术重点实验室, 福建 福州 350007

摘要 非共线声光可调滤波器(AOTF)是一种利用反常声光作用原理制成的新型分光器件,其衍射信号的光谱分辨率和旁瓣是评价AOTF性能的两个重要指标。阐述了通过两个AOTF进行二次滤波的基本原理。实验证实了二次滤波法可使AOTF衍射信号的光谱分辨率提高40.4%~3.2%和旁瓣抑制9.5570 dB到13.2407 dB。研究结果表明用两个AOTF进行二次滤波在声光滤波领域有着巨大的应用前景。

关键词 光学器件; 声光可调滤波器; 光谱分辨率; 旁瓣; 二次滤波

中图分类号 O439 **文献标识码** A

doi: 10.3788/LOP52.092301

1 Introduction

The noncollinear acousto-optic tunable filter (AOTF) is a new type of spectral component that is developed according to the abnormal acousto-optic interaction principle. The design and production of AOTFs are convenient, because AFTOs do not require the collineation of incident light wave vectors and ultrasound wave vectors. Meanwhile, compared with conventional spectroscopic devices, AOTFs exhibit advantages such as small volume, rapid tuning, large aperture angle, high diffraction efficiency, narrow band pass and so on. Therefore, AOTFs have potential applications in many areas, including rapid spectral analysis, optical image processing, environmental monitoring, optical computing, wavelength division multiplexing and spectral imaging[1-10].

However, compared with the linear AOTF, the noncollinear AOTF exhibits a low spectral resolution. The

收稿日期: 2015-01-27; **收到修改稿日期**: 2015-02-27; **网络出版日期**: 2015-08-12

基金项目: 国家自然科学基金(61107092),福建师范大学青年骨干教师资助计划(fjsdjk2012055)

作者简介: 黄峻峰(1987—),男,硕士研究生,主要从事声光技术方面的研究。E-mail: jfhuang668@qq.com

导师简介: 王 号(1978—),男,博士,副教授,主要从事声光技术、超光谱成像以及非线性光学等方面的研究。E-mail: haowang@fjnu.edu.cn

spectral resolution is one of main indices for evaluating the performance of designed AOTF. Therefore, it is a trending research area, and there is great demand to improve the spectral resolution of noncollinear AOTFs for various applications. In addition, the diffraction signal spectrum after filtering has evident sidelobes because the system affects the purity of the diffraction signal. On the basis of the TeO_2 crystal characteristics, an efficient double-filtering technique employing two AOTFs is developed. Double-filtering is investigated as a method to improve the spectral resolution of AOTFs and curb the sidelobes of the diffraction signal spectrum.

2 Design of Experiment

The principle of the double-filtering is shown in Fig.1. Considering the rotatory property, two AOTFs are employed[11-12]. The design parameters and performance indices of $AOTF_1$ and $AOTF_2$ are listed in Table 1.

Table 1 Design parameters and performance indices of $AOTF_1$ and $AOTF_2$

Item	$AOTF_1$	$AOTF_2$
Working waveband /nm	400~700	400~700
Frequency tuning range /MHz	107.5~223.5	107.5~223.5
Incident polar angle /(°)	23.80	21.17
Diffraction polar angle /(°)	21.17	23.80
Spectral resolution	218.5 @ 632.8 nm	174.9 @ 632.8 nm
Optical wedge angle /(°)	6.15	6.50

Two AOTFs are placed on an optical platform, ensuring that the two principal planes of the TeO_2 crystals are parallel. The piezoelectric transducer and sound absorber of the AOTF are bonded on its anterior and posterior surfaces, respectively. The radio-frequency source of the piezoelectric transducer is selected to realize the rapid electronic tuning of the AOTFs, thus the ultrasonic frequencies of signals passing through the AOTFs are changed.

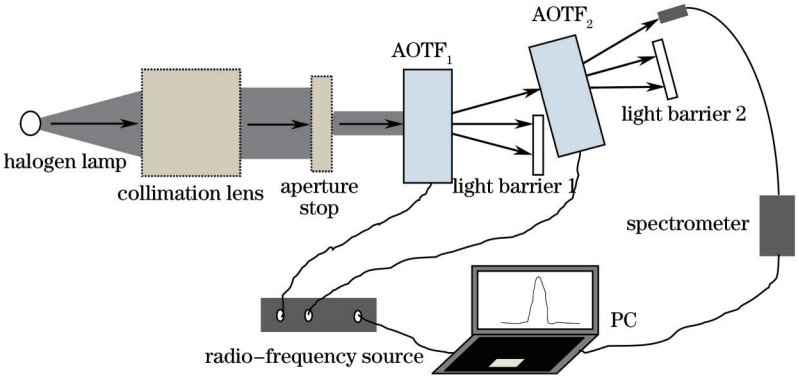

Fig.1 Principle of double-filtering

A halogen lamp with the wavelength range of 400~1000 nm is chosen as the light source. After passing through the collimation lens and the aperture stop, the light is parallel. The parallel light is perpendicularly incident on the crystal surface of the first AOTF ($AOTF_1$), and it is divided into three beams: the positive and negative first levels of the diffractive light and the non-diffractive light due to Bragg diffraction. The negative first level of the diffractive light and the non-diffractive light are removed using a light barrier, so that the spectrometer only receives the positive first level of the diffractive light. After being collected by the spectrometer, the positive first level of the diffractive light is incident on the crystal surface of the second AOTF ($AOTF_2$). Then, the light passing through $AOTF_2$ is divided into three beams, and the spectrometer receives only the positive first level of the diffractive light, as the other light is blocked by the light barrier.

The experimental platform is configured according to the aforementioned double-filtering principle. Subsequently, a single-filtering experiment is performed. We set the frequency of the ultrasonic signal

of AOTF$_1$, f_{a1}, as 110, 120, 130, 140 and 150 MHz. The spectrometer only receives the positive first level of the diffractive light. The central wavelength λ_{10} and spectral bandwidth $\Delta\lambda_1$ of the diffractive light are recorded by the spectrometer software. Next, the diffracted light is measured when the light passes through AOTF$_2$, and it is convenience to compare the single-filtering and double-filtering. During the experiment, f_{a1} is kept constant and f_{a2} is changed in the range of f_{a2} -0.5 MHz to f_{a2} +0.5 MHz every other 0.01 MHz. After the double-filtering, the diffractive spectrum of the light is collected and the central wavelength λ_{20} and spectral bandwidth $\Delta\lambda_{12}$ are recorded.

3 Results and Discussion

Fig.2 shows the single-filtering and double-filtering spectral contrast under the ultrasound frequency of f_{a1} = 130 MHz. Each frame contains two spectrums. The black and red curves are the diffractive light spectra of the single-filtering and double-filtering, respectively. They are labeled AOTF1 and AOTF12, respectively.

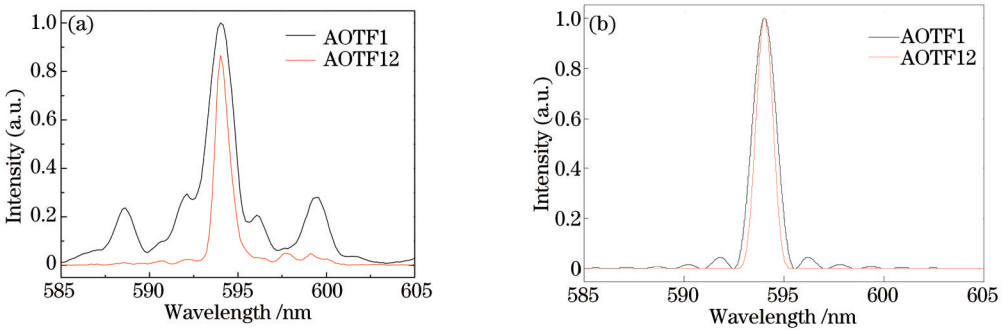

Fig.2 Spectral comparison between single-filtering and double-filtering under f_{a1} = 130 MHz. (a) Experimental results; (b) theoretical results

The black spectrum (AOTF1) in Fig.2(a) shows that there are sidelobes on either side of the main peak of the diffractive light for the single-filtering. The first sidelobe is the most obvious. We set the main peak's maximum value as 0 dB, and the maximum values of the first sidelobes on either side are -6.2478 dB and -5.5210 dB, respectively (the maximum intensities of the first sidelobes on either side are 0.23726 and 0.28048, respectively). The red spectrum (AOTF12) shown in Fig.2(a) is recorded by changing f_{a2} in the double-filtering experiment while maintaining f_{a1} = 130 MHz, so that the diffraction light center wavelength λ_{20} equals the single-filtering experiment value λ_{10}. The maximum values of the first sidelobes on either side are -19.4885 dB and -15.0780 dB, respectively (their maximum intensities are 1.125×10^{-2} and 3.106×10^{-2}, respectively). The first sidelobes of the single-filtering diffractive light are suppressed, and their values are respectively reduced by 13.2407 dB and 9.5570 dB through the double-filtering. The results clearly indicate that double-filtering is effective for controlling the sidelobes of diffraction spectrums, confirming the findings of previous studies[13-14].

The theoretical calculation results are shown in Fig.2(b). As indicated by the black spectrum (AOTF1), sidelobes are observed on either side of the main peak of the diffractive light for the single-filtering. The maximum values of the first sidelobes on either side are both -13.2615 dB (the maximum intensities are both 4.719×10^{-2}). The red spectrum (AOTF12) in Fig.2(b) shows the results for double-filtering. The maximum values of the first sidelobes on either side are both -26.5228 dB (the maximum intensities are both 2.227×10^{-3}). According to the comparative data and aforementioned spectra, the theoretical and experimental results exhibit similar center wavelengths and spectral bandwidths at equal ultrasonic frequency. However, the experimental values of the sidelobes are 6 dB greater than the theoretical values. The obvious sidelobes observed experimentally may arise from three aspects: the effect of the optical collimated system before AOTF[15], the material characteristics of the TeO_2 crystals, and the quality of the ultrasonic signals. The

sidelobes can affect the AOTF performance, thus they must be controlled according to the three aforementioned factors. Fig.2(a) shows that the diffraction efficiency of the diffractive light decreases by 13.4% after the double-filtering in our experiment. In contrast, Fig.2(b) shows that the intensity of the diffractive light is unchanged. In theory, considering the same two spectral peaks that are respectively achieved by $AOTF_1$ and $AOTF_2$, the diffraction efficiency can reach 100% when the two peaks overlap. However, in the experiment, the two main peaks achieved by $AOTF_1$ and $AOTF_2$ are inconsistent, yielding an overlap between one spectrum's peak and the other's off-peak. Ultimately, the experimental diffraction efficiency is 86.6%.

Table 2 Single-filtering and double-filtering data at different ultrasound frequencies

f_{a1} /MHz	$\lambda_{10}=\lambda_{20}$ /nm	$\Delta\lambda_1$ /nm	$\Delta\lambda_{12}$ /nm	$R_1=\lambda_{10}/\Delta\lambda_1$	$R_{12}=\lambda_{20}/\Delta\lambda_{12}$
110	679.55	1.91	1.19	355.79	571.05
120	632.83	1.60	1.14	395.52	555.11
130	594.05	1.74	0.95	341.41	625.31
140	560.73	1.31	0.76	428.04	737.80
150	539.40	1.09	0.67	494.86	805.07

Table 2 indicates that the diffraction signal's spectral width for single-filtering, $\Delta\lambda_1$, is smaller than that for double-filtering, $\Delta\lambda_{12}$, at various ultrasonic frequencies. Calculations indicate that $\Delta\lambda_{12}$ is 37.7%, 28.8%, 45.4%, 42.0%, and 38.5% smaller than $\Delta\lambda_1$ when f_{a1} is 110, 120, 130, 140, and 150 MHz, respectively. The spectral resolution of the AOTF can be expressed by the specific value of the central wavelength λ_0 and the spectral width $\Delta\lambda$ of the diffractive light, that is, $\lambda_0/\Delta\lambda$. The spectral resolution for double-filtering is 60.5%, 40.4%, 83.2%, 72.4%, and 62.7% higher than that for single-filtering at the respective ultrasonic frequencies. These data fully demonstrate that double-filtering is effective for enhancing the spectral resolution of AOTFs.

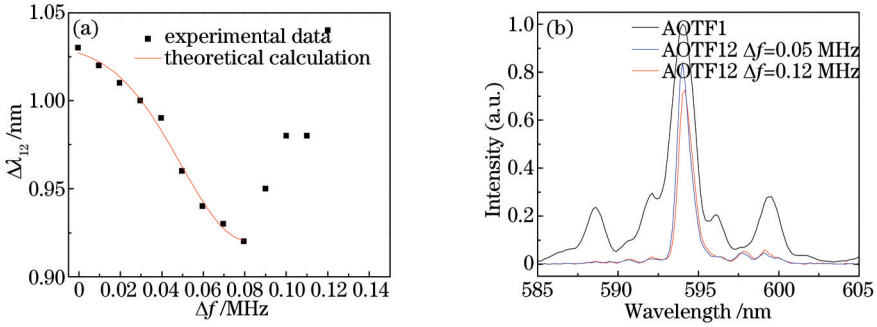

Fig.3 (a) Double-filtering spectral width $\Delta\lambda_{12}$ as a function of ultrasonic frequency difference Δf when f_{a1} = 130 MHz; (b) comparison among single-filtering spectrum and double-filtering spectra for Δf = 0.05 and 0.12 MHz when f_{a1} = 130 MHz

Finally, the behavior of the double-filtering spectral width, $\Delta\lambda_{12}$, is analyzed by changing the value of $\Delta f=f_{a1}-f_{a2}$ while keeping f_{a1} constant. Fig.3(a) shows $\Delta\lambda_{12}$ varies as a function of Δf when f_{a1} = 130 MHz. As Δf increases, $\Delta\lambda_{12}$ first decreases and then increases. The minimum $\Delta\lambda_{12}$ is achieved when Δf = 0.08 MHz. The downward trend of $\Delta\lambda_{12}$ in the first half of the plot agrees well with the theoretical analysis. The upward trend in the latter half may be related to the sidelobes of AOTF1, which are shown in Fig.3(b). Therefore, during the double-filtering experiment, the spectral width of the light can be accurately selected from the measured target by changing the value of f_{a2} while keeping f_{a1} constant, thereby the spectral resolution is enhanced.

4 Conclusion

An efficient double-filtering technique employing two AOTFs is proposed to enhance the spectral

resolution of AOTFs. Compared with single-filtering, double-filtering is more effective for controlling the sidelobes to remove unwanted spectral components. Moreover, double-filtering can reduce the spectral width of diffraction signals, thereby effectively enhancing the spectral resolution of AOTFs. The selection of the ultrasonic frequency in the double-filtering experiment is examined. According to the experimental results, the double- filtering technology comprising two AOTFs can effectively enhance the spectral resolution by 40.4%~83.2%. It also reduces the sidelobes of the AOTFs′ diffractive signals by 9.5570 dB~13.2407 dB . Therefore, this technology has potential for application in the field of acousto-optic filtering.

References

1 Chang Lingying, Zhao Baochang, Qiu Yuehong, *et al.*. Optical design of imaging spectrometer based on acousto-optic tunable filter[J]. Acta Optica Sinica, 2010, 30(10): 3021-3026.
常凌颖, 赵葆常, 邱跃洪, 等. 声光可调谐滤波器成像光谱仪光学系统设计[J]. 光学学报, 2010, 30(10): 3021-3026.

2 MiranBürmen, FranjoPernuš, BoštjanLikar. Spectral characterization of near- infrared acousto- optic tunable filter (AOTF) hyperspectral imaging systems using standard calibration materials[J]. Applied Spectroscopy, 2011, 65(4): 393-401.

3 Yu Yang, Xuejun Sha, Zhonghua Zhang. Analysis of the deviation of the diffracted beams caused by acousto- optic tunable filter in multispectral imaging[J]. Chin Opt Lett, 2011, 9(8): 081101.

4 Xiong Shengjun, Zhang Ying, Zhao Huijie, *et al.*. Aspheric optical design of an imaging spectrometer based on acousto-optic tunable filter[J]. Acta Optica Sinica, 2012, 32(6): 0622002.
熊胜军, 张 颖, 赵慧洁, 等. 声光可调滤波器成像光谱仪非球面光学系统设计[J]. 光学学报, 2012, 32(6): 0622002.

5 Emmanuel Dekemper, Nicolas Loodts, Bert Van Opstal, *et al.*. Tunable acousto-optic spectral imager for atmospheric composition measurements in the visible spectral domain[J]. Appl Opt, 2012, 51(25): 6259-6267.

6 Rula Tawalbeh, David Voelz, David Glenar, *et al.*. Infrared acousto-optic tunable filter point spectrometer for detection of organics on mineral surfaces[J]. Optical Engineering, 2013, 52(6): 063604.

7 Wang Xiwei, Zhao Maocheng, Ju Ronghua, *et al.*. Visualizing quantitatively the freshness of intact fresh pork using acousto-optical tunable filter-based visible/near-infrared spectral imagery[J]. Computers and Electronics in Agriculture, 2013, 99: 41-53.

8 Neelam Gupta, Vitaly B Voloshinov, Gregory A Knyazev, *et al.*. Optical transmission of single crystal tellurium for application in acousto-optic cells[J]. Journal of Optics, 2011, 13(5): 055702.

9 Zhang Wending, Huang Ligang, Gao Feng, *et al.*. Tunable broadband light coupler based on two parallel all- fiber acousto-optic tunable filters[J]. Opt Express, 2013, 21(14): 16621-16628.

10 Zhang Chunguang, Wang Hao, Gao Qiang, *et al.*. Application of acousto-optic tunable technology on palm skin spectral imaging[J]. Chinese J Lasers, 2014, 41(s1): s116006.
张春光, 王 号, 高 强, 等. 声光可调滤波技术在人掌皮组织光谱成像上的应用[J]. 中国激光, 2014, 41(s1): s116006.

11 Zhang Chunguang, Zhang Zhonghua, Wang Hao, et al.. Analysis of the optimum optical incident angle for an imaging acousto-optic tunable filter[J]. Opt Express, 2007, 15(19): 11883-11888.

12 Wang Hao, Zhang Chunguang, Huang Junfeng, *et al.*. Design and performance evaluation of a narrow band acousto-optic filter considering the rotatory property[J]. Acta Optica Sinica, 2014, 34(4): 0423002.
王 号, 张春光, 黄峻峰, 等. 考虑旋光影响的窄带声光滤波器设计及其性能分析[J]. 光学学报, 2014, 34(4): 0423002.

13 Zhang Chunguang, Zhang Zhonghua, Wang Hao, *et al.*. Spectral resolution enhancement of acousto-optic tunable filter by double filtering[J]. Opt Express, 2008, 16(14): 10234-10239.

14 J W You, J Ahn, S Kim, *et al.*. Efficient double-filtering with a single acousto-optic tunable filter[J]. Opt Express, 2008, 16(26): 21505-21511.

15 D Voelz, B Kodali. Characterization of an acousto-optic tunable filter imaging system[C]. SPIE, 2006, 6302: 62020p.

栏目编辑：刘丰瑞